Near-field excitation and near-field detection of propagating surface plasmon polaritons on Au waveguide structures

R. Dallapiccola,[1] C. Dubois,[1] A. Gopinath,[2] F. Stellacci,[1,a)] and L. Dal Negro[2,3]
[1]*Department of Materials Science and Engineering, Massachusetts Institute of Technology, 77 Massachusetts Avenue, Cambridge, Massachusetts 02139, USA*
[2]*Department of Electrical and Computer Engineering, Boston University, Boston, Massachusetts 02215, USA*
[3]*Division of Materials Science and Engineering, Boston University, Brookline, Massachusetts 02446, USA*

(Received 17 March 2009; accepted 18 May 2009; published online 19 June 2009)

The propagation of surface plasmon polaritons guided along Au metal waveguides fabricated by electron-beam lithography is experimentally investigated using simultaneous near-field excitation and detection of plasmon-polariton modes localized at the air/Au interface. The directly measured propagation characteristics of surface plasmon-polaritons agree well with simulation results obtained using full-vector calculations and the analytic dispersion of asymmetric plasmonic waveguides for thin Au films. Our results demonstrate that near-field excitation/detection schemes are well suited for direct imaging and characterization of propagating surface plasmon-fields bound to thin-film metal layers, and can be used for fast and reliable characterization of plasmonic waveguide elements and nanodevices. © *2009 American Institute of Physics*.
[DOI: 10.1063/1.3152291]

The possibility to control subwavelength light propagation along metal-dielectric interfaces offers the ultimate potential for miniaturized, high-speed optoelectronic devices operating beyond the classical diffraction limit.[1,2] Subdiffractive light guiding using surface plasmon polaritons (SPPs) at metal-dielectric interfaces[3,4] and near-field coupling in nanoparticle metal chains[5] are central in the field of nanoplasmonics, which is concerned with the manipulation of subwavelength optical fields on planar chips. In particular, nanoscale optical devices such as plasmonic waveguides[4–7] and metal slots,[8,9] bandgap structures,[10] and optical nanoantennas[11] have been recently demonstrated. As a result, the demand for fast and reliable techniques for the imaging of nanoscale optical fields is consistently growing. In particular, efficient near-field excitation and imaging schemes are needed in order to quantitatively investigate the transport characteristics of SPP waves guided along metal-dielectric interfaces. SPPs are surface waves coupled to free electron oscillations in metals. Due to their ability to strongly enhance the field intensity at metal/dielectric interfaces, SPPs are key elements in optical sensing and are expected to play a major role in future nanoplasmonic integration.[1] An important feature of SPPs is that their wave vector is always larger than the one of light in free space. As a result, the optical excitation of SPP waves is only possible if the wave vector of the exciting light is increased over its free space value. Several experimental methods have been developed to achieve this goal: far-field excitation using grating coupling or attenuated total reflection (ATR), and near-field excitation using localized sources, as in near-field scanning optical microscopy (NSOM).[2,12]

The most commonly used configuration for the study of the SPPs propagation characteristics is far-field illumination and near-field detection, in which SPPs are excited using strongly focused beams, diffraction gratings, or ATR prisms, and detected in the near-field using either a photon scanning tunneling microscope[13] or a NSOM. To date, a scheme based on direct near-field excitation and near-field detection of SPP waves on a metal film still remains to be investigated.

In this paper, we demonstrate the feasibility of a two-tip near-field excitation/detection scheme for the study of the propagation characteristics of SPPs waves on Au waveguides on Si. In particular, based on three-dimensional (3D) finite difference time domain (FDTD) calculations, we discuss the optimal conditions which lead to the determination of the SPP propagation length and minimize the undesired coupling between the excitation and the detection probes.

We fabricated plasmonic waveguides using electron beam lithography on *p*-type silicon wafers. A 180 nm thick PMMA 950 (polymethyl methacrylate) film was spin coated on top of the substrate. Subsequently, plasmonic waveguides were defined using a Zeiss SUPRA 40VP scanning electron microscopy (SEM). The resist was developed in methyl isobutyle ketone and a Au film with a thickness of 55 nm was deposited on the patterned surface by electron-beam evaporation. Au waveguides on Si were obtained after the lift off process performed in acetone. A top view SEM image of the investigated waveguide sample is also shown in Fig. 1. The near-field optical measurements were performed using a MultiView™ 3000 scanning dual probe microscope/NSOM system (Nanonics Imaging Ltd., Jerusalem, Israel). A schematics of the configuration used for the two-tip experiment is shown in Fig. 1. The scanning probe microscope (SPM) head allows for simultaneous atomic force microscopy (AFM) and NSOM imaging. The plasmonic waveguide sample was locally excited at 528.7 nm (Ar:Kr laser, Coherent, Innova 70C Spectrum) using a single mode polarization maintaining fiber terminated by a cantilevered aperture Cr–Au coated NSOM probe (0.02 and 0.2 μm) with 300 nm in diameter. The illumination probe approached the waveguide approximately 6 μm away from the end of the narrow metal strip that we

[a)]Author to whom correspondence should be addressed. Electronic mail: frstella@mit.edu.

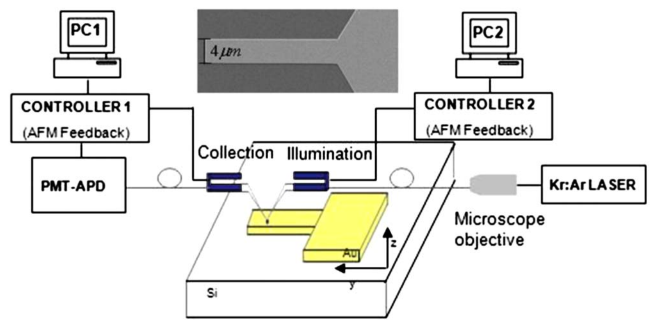

FIG. 1. (Color online) Schematic of the experimental setup for the near-field excitation and near-field detection of SPP waves at metal-air interface and the top view SEM image of the plasmonic waveguide studied in this paper.

were testing as waveguide. The distance and the position of this probe were determined by first using this probe as an AFM tip and acquiring an image of the sample and then locking it in the desired place. A similar 200 nm width aperture NSOM probe was scanned above the sample in collection mode to measure the field intensity associated with the radiative decay of the propagating SPP wave, which was finally collected onto a photomultiplier tube (MP900, PerkinElmer Optoelectronics, Fremont, USA). In order to assure that the probes were in contact with the sample surface, an initial AFM scan of the sample was performed, first with the illumination probe and then with the collection one. Both tips were operated using a tuning fork shear-force feedback.

Figure 2(a) shows the AFM image of the end facet of the plasmonic waveguide. The measured root mean squared

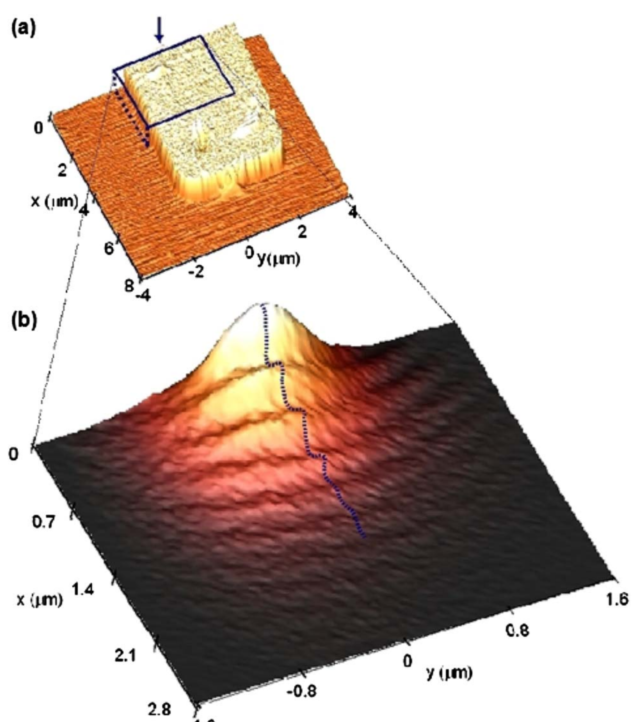

FIG. 2. (Color online) (a) 3D rendering of an AFM topography (8 μm^2) image of the extremity of the waveguide. The arrow indicates the position of the illumination probe. (b) 3D rendering of the NSOM signal, acquired in the area delimited by the rectangle in (a), showing the SPP oscillation pattern with exponential attenuation (acquisition time=50 min). The image is obtained by laterally averaging the NSOM intensity profile over five pixels (i.e., ± 30 nm) along the waveguiding x-axis measured from the signal maximum [dashed blue line as a guide for the eye in Fig. 2(b)].

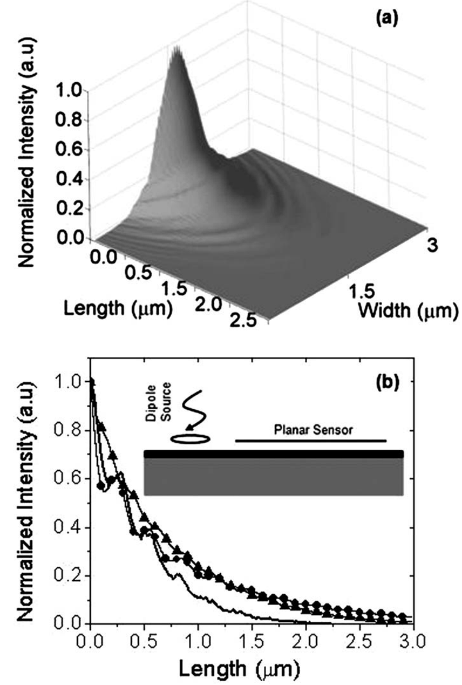

FIG. 3. (a) 3D FDTD calculation of SPP intensity propagation. (b) (solid line) Experimental intensity decay along the waveguide. FDTD simulations of the intensity decay of the SPP obtained using the geometry shown in the inset for a sample-probe separation of 5 nm (circles, solid line) and 25 nm (triangles, solid line).

roughness was 2.3 nm, limited by PMMA residual particles from the lift off process. The arrow indicates the location of the illumination probe at the upper edge of the AFM image. High-resolution NSOM images have been acquired close to the illumination probe in a 3.2×2.8 μm^2 area [rectangle in Fig. 2(a)]. During the measurements, the collection probe was scanning the sample area while approaching the illumination probe. In order to avoid any mechanical coupling between the two probes, the image acquisition was stopped when the collection probe was imaging the illumination probe, as directly seen in the AFM acquisition window. Under this condition, the minimum distance between the two probes is approximately the sum of the two aperture radii and coating thicknesses (690 nm).

A sudden decrease in the scattered signal intensity was observed when vertically (z-direction) retracting the collection probe, as expected for SPP modes, which are exponentially bound to the metal-air interface. Indeed, the signal fully vanished when the collection probe was retracted by 100 nm from the surface of the sample.

Figure 2(b) shows the near-field intensity (NSOM) image taken at 528.7 nm excitation for the same waveguide region as in Fig. 2(a). This image shows the measured intensity profile of the SPP wave propagating at the top interface of the waveguide. A pattern of oscillations with an exponentially damping intensity can be readily observed in Fig. 2(b). Recently, intensity oscillations in the SPPs propagation have been reported and explained as due to either plasmonic mode interference[14] or multiple reflections from the waveguide facets.[15] In order to explain the signal oscillations observed in our experimental configuration, we performed FDTD simulations of the experimental geometry.[16] The geometry of the calculation is sketched in the inset of Fig. 3(b). FDTD simulations were performed using a p-polarized point dipole source at 528.7 nm, and a mesh size of 2 nm was used. Figure 3(a) shows the surface plot of the calculated intensity profile. For the optical parameters of Au at 528.7 nm we used $n=0.6-2.0i$.[17] The calculations clearly reveal an intensity oscillation pattern, in good agreement with the experimental data shown in Fig. 2(b). Both the experimental and the calculated oscillation patterns have a periods corresponding to the excitation wavelength of the source. These data therefore demonstrate coupling effects between the propagating components of the excitation and the detection fields.

In order to better understand these coupling effects, we performed FDTD calculations considering tips located at two different heights (5 and 25 nm) above the top surface of the Au waveguide. To reproduce the experimental geometry, a minimum distance of 690 nm was considered between the excitation source and the extended FDTD sensor, which evaluates the electric field intensity propagating along the waveguide axis. The circles and triangles—solid lines in Fig. 3(b)—show the calculated intensity profiles assuming a sample-probe distance of 5 and 25 nm, respectively.

The results shown in Fig. 3(b) demonstrate that the vertical tip position affects their coupling efficiency. This coupling in turn perturbs the spatial decay of the SPP wave. In particular, our results show that the SPPs propagation length can be significantly perturbed by the two-tip experimental geometry, especially when using large aperture tips (~200 nm). This is reinforced by comparing with the predictions of analytical waveguide theory for SPP waves. For three-layer asymmetric plasmonic waveguides, a simple theory exists for the calculation of the complex SPP propagation constant β, from which the wavelength and the SPP propagation length can be obtained.[18] This can be done by numerically finding the complex poles of the SPP dispersion relation:[18]

$$\tanh(S_2h)(\varepsilon_1\varepsilon_3S_2^2+\varepsilon_m^2S_1S_3)+[S_2(\varepsilon_1S_3+\varepsilon_3S_1)\varepsilon_m]=0, \tag{1}$$

where $S_i^2=\beta^2-\varepsilon_ik_0^2$ and $\varepsilon_i=n_i^2$ are the dielectric functions of the materials, and h is the thickness of the metal layer sandwiched between the two dielectrics (air, Si). Once the solutions of Eq. (1) have been found, the SPP wavelength follows as $\lambda_{SPP}=2\pi/\mathrm{Re}(\beta)$, and the SPPs extinction length as $\ell_{SPP}=1/2\ \mathrm{Im}\ \beta$. Using Eq. (1) with the experimental parameters $h=55$ nm, $n_1=3.5$, $n_2=0.6-i2.0$, and $n_3=1.0$, we obtain $\ell_{SPP}\approx 652$ nm. This result very well agrees with the FDTD estimated propagation length of SPP waves ($\ell_{SPP}\approx 630$ nm) in the limit of very small (5 nm) probe sample separation. On the other hand, the measured SPP decay length (Fig. 3, solid line) is $\ell_{SPP}\approx 550$ nm. The shorter SPP propagation length experimentally measured could be explained by a deviation of the actual optical constants with respect to the ones used in the calculations and by the additional scattering losses in the sample. Therefore, our analysis indicates that the two-tip technique can be used to roughly estimate the SPPs propagation length and therefore the intrinsic losses of plasmonic waveguides if the two tips are in close contacts (few nanometers) with the sample. However, from Eq. (1) we obtain $\lambda_{SPP}=2\pi/\mathrm{Re}(\beta)\approx 460$ nm. Therefore, the measured intensity oscillations, which occur at approximately 530 nm, are due to the optical coupling of the two tips, which modulates the SPP intensity at a frequency corresponding to the excitation source. This "stray coupling effect" is also visible in the FDTD simulations in Fig. 3, which demonstrate how the intensity oscillations depend on the tip sample distance and reduce when this distance is 5 nm. Therefore, our combined experimental and computational analysis demonstrate that optical coupling between the two tips results in undesired oscillations at the pump frequency, which can only be eliminated when operating the tips in close proximity to the sample's surface. Under these conditions, we have shown that the proposed two-tip technique provides a good estimate of the SPP propagation length.

In summary, we demonstrated and discussed the validity of a near-field excitation, near-field detection two-tip measuring technique suitable for the determination of propagation length in plasmonic waveguides. Based on FDTD simulations and the analytical theory of plasmonic waveguides, we discussed the effects of tips coupling and we directly imaged the free propagation of SPPs modes on asymmetric Au/Si waveguides.

F.S. acknowledges the support of the Packard Foundation and the valuable help of Nanonics.

[1] *Surface Plasmon Nanophotonics*, edited by M. L. Brongersma and P. G. Kik (Springer, Dordrecht, 2007).
[2] D. W. Pohl, W. Denk, and M. Lanz, Appl. Phys. Lett. **44**, 651 (1984).
[3] J. R. Krenn and J. C. Weeber, Philos. Trans. R. Soc. London, Ser. A **362**, 739 (2004).
[4] R. Zia, J. A. Schuller, and M. L. Brongersma, Phys. Rev. B **74**, 165415 (2006).
[5] M. L. Brongersma, J. W. Hartman, and H. A. Atwater, Phys. Rev. B **62**, R16356 (2000).
[6] S. A. Maier, P. G. Kik, H. A. Atwater, S. Meltzer, E. Harel, B. E. Kohel, and A. Requicha, Nature Mater. **2**, 229 (2003).
[7] R. Zia, J. A. Schuller, A. Chandran, M. L. Brongersma, Mater. Today **9**, 20 (2006).
[8] J. A. Dionne, L. A. Sweatlock, H. A. Atwater, and A. Polman, Phys. Rev. B **73**, 035407 (2006).
[9] N.-N. Feng, M. L. Brongersma, and L. Dal Negro, IEEE J. Quantum Electron. **43**, 479 (2007).
[10] S. I. Bozhevolnyi, J. Erland, K. Leosson, P. Skovgaard, and J. M. Hvam, Phys. Rev. Lett. **86**, 3008 (2001).
[11] P. Muhlschlegel, H. J. Eisler, O. J. F. Martin, B. Hecht, and D. W. Pohl, Science **308**, 1607 (2005).
[12] A. Lewis, M. Isaacson, A. Harootunian, and A. Muray, Ultramicroscopy **13**, 227 (1984).
[13] I. I. Smolyaninov, D. L. Mazzoni, J. Mait, and C. C. Davis, Phys. Rev. B **56**, 1601 (1997).
[14] E. Verhagen, J. A. Dionne, L. Kuipers, H. A. Hatwater, and A. Polman, Nano Lett. **8**, 2925 (2008).
[15] J. C. Weeber, J. R. Krenn, A. Dereux, B. Lamprecht, Y. Lacroute, and J. P. Goudonnet, Phys. Rev. B **64**, 045411 (2001).
[16] OMNISIM software by Photon Design, Oxford, UK.
[17] P. B. Johnson and R. W. Christy, Phys. Rev. B **6**, 4370 (1972).
[18] J. J. Burke, G. I. Stegeman, and T. Tamir, Phys. Rev. B **33**, 5186 (1986).